AFRPL-TR-81-55

AN ANALYSIS OF A SOLID PROPELLANT TRANSIENT VISCOELASTIC RESPONSE UNDER MOTOR IGNITION CONDITIONS

Authors: Durwood I. Thrasher
Eileen Corbett

January 1982

Final report for the period 9 July 1980 to 15 April 1981

APPROVED FOR PUBLIC RELEASE; DISTRIBUTION UNLIMITED

The AFRPL Technical Services Office has reviewed this report, and it is releasable to the National Technical Information Service, where it will be available to the general public, including foreign nationals.

Prepared for

AIR FORCE ROCKET PROPULSION LABORATORY
DIRECTOR OF SCIENCE AND TECHNOLOGY
AIR FORCE SYSTEMS COMMAND
EDWARDS AFB, CALIFORNIA 93523

NOTICES

FOREWORD

This report describes the work conducted by the Mechanical Behavior and Aging Section (MKPB) of the Air Force Rocket Propulsion Laboratory, Edwards AFB, California 93523 under Job Order No. 2307M1MD.

This Technical Report is approved for release and distribution in accordance with the distribution statement on the cover and on the DD Form 1473.

Durwood I. Thrasher

DURWOOD I. THRASHER
Project Manager

R. John Moss

R. JOHN MOSS, Capt, USAF
Chief, Mechanical Behavior and Aging Section

FOR THE DIRECTOR

Charles R. Cooke

CHARLES R. COOKE
Director, Solid Rocket Division

UNCLASSIFIED

SECURITY CLASSIFICATION OF THIS PAGE (When Data Entered)

REPORT DOCUMENTATION PAGE		READ INSTRUCTIONS BEFORE COMPLETING FORM
1. REPORT NUMBER AFRPL-TR-81-55	2. GOVT ACCESSION NO. AD-A114 345	3. RECIPIENT'S CATALOG NUMBER
4. TITLE (and Subtitle) An Analysis of Solid Propellant Transient Viscoelastic Response Under Motor Ignition Conditions		5. TYPE OF REPORT & PERIOD COVERED Final Report 9 Jul 80 to 15 Apr 81
		6. PERFORMING ORG. REPORT NUMBER
7. AUTHOR(s) Durwood I. Thrasher Eileen Corbett		8. CONTRACT OR GRANT NUMBER(s)
9. PERFORMING ORGANIZATION NAME AND ADDRESS Air Force Rocket Propulsion Laboratory (MKPB) Edwards AFB CA 93523		10. PROGRAM ELEMENT, PROJECT, TASK AREA & WORK UNIT NUMBERS Project 573013 MD
11. CONTROLLING OFFICE NAME AND ADDRESS		12. REPORT DATE January 1982
		13. NUMBER OF PAGES 33
14. MONITORING AGENCY NAME & ADDRESS(if different from Controlling Office)		15. SECURITY CLASS. (of this report) UNCLASSIFIED
		15a. DECLASSIFICATION/DOWNGRADING SCHEDULE

16. DISTRIBUTION STATEMENT (of this Report)

Approved for Public Release; Distribution Unlimited

17. DISTRIBUTION STATEMENT (of the abstract entered in Block 20, if different from Report)

18. SUPPLEMENTARY NOTES

19. KEY WORDS (Continue on reverse side if necessary and identify by block number)

Solid Rocket Propellants
Solid Propellant Mechanical Behavior
Sinear Viscoelasticity
Transient Loading
Motor Ignition Pressurization
Motor Structural Analysis

20. ABSTRACT (Continue on reverse side if necessary and identify by block number)

Programmable calculator programs were written to calculate stress responses for stepwise and rampwise approximations to a given strain history. These programs were tailored to calculate the error relative to the exact-history result and also to investigate different techniques of applying stepwise approximations and different techniques for selecting stress output times within each step or ramp. The optimum rampwise approximation produced one-tenth the rms error in stress produced by the optimum stepwise approximation for the same

DD FORM 1 JAN 73 1473 EDITION OF 1 NOV 65 IS OBSOLETE

UNCLASSIFIED

SECURITY CLASSIFICATION OF THIS PAGE (When Data Entered) number of time intervals. Using only 10 time intervals to approximate a fourth-order polynomial strain history, the rms error in stress with the rampwise approximation was only 0.5%. The ramowise approximation program was then rewritten for analysis of an arbitrary input strain history (up to 35 ramps). A dynamic pressurization-strain test reported in AFRPL-TR-78-68 was analyzed using the rampwise strain history approximation as well as a polynomial approximation. For both strain history approximations, the stress history calculated using relaxation data agreed well with the measured stress history up to the peak stress point. The error at peak stress for both approximations was less than 20 psi, or roughly 2.5% of the measured value of 810 psi. This is considered excellent agreement with the experimental data.

TABLE OF CONTENTS

LIST OF FIGURES

LIST OF FIGURES (concluded)

LIST OF TABLES

1. INTRODUCTION

The objective of this project was to evaluate two alternative approaches (step approximation of strain history and ramp approximation of strain history) to calculating the transient stress response of a linear viscoelastic material to an arbitrary strain-time input, and to determine the better approach for calculating effective modulus for motor ignition pressurization from stress relaxation data.

The project began with the plan of expanding the capability of an existing programmable calculator program which calculates stress response to piecewise-linear strain histories so that it could handle at least 20 individual constant-strain-rate segments. This program would then be used to calculate stress response using both a series of step functions and a series of ramp functions to approximate a specific "exact" continuous-slope transient strain history.

It was found that writing new calculator programs was more effective than expanding the old program. One of these new programs can handle a piecewise-linear strain history consisting of up to 50 constant-strain-rate segments (however, only 35 ramps can be loaded from the tape data file in the present data format). Other calculator programs (discussed later in this report) were written to perform specific calculations.

A study was made to refine the methods of approximating the strain history in each approach. To determine the accuracy of the stress response, the stress responses were compared with the exact solution for a specific transient strain history.

2. SUMMARY

The modified power law representation of relaxation modulus is amenable to straightforward calculation of linear viscoelastic response to a constant rate (ramp) strain input. A piecewise-linear function can approximate a complex strain history with reasonable accuracy. This piecewise-linear function is merely the sum of a series of ramp functions; the response of the material to the piecewise-linear strain history is, in turn, simply the summation of the responses to the individual ramps.

This concept was applied successfully in the analyses described in this report. The rms error in calculated stress using as few as 10 ramps to approximate a fourth-order-polynomial strain history (quite similar to the strain history typically produced by motor ignition pressurization) is shown to be less than 0.5%. This accuracy is superior to that obtained with 100 steps in the usual stepwise approximation.

The technique was also applied to actual propellant data from low temperature, high rate transient tests in which the propellant strain was driven by a pressure dynamically applied to a fluid surrounding the test specimens. Using stress relaxation data the calculated stress agrees with the measured stress within 2.5% at peak stress. This excellent agreement provides evidence that linear viscoelasticity may be successfully applied to the ignition pressurization problem, although the problem of prestrain effects was not addressed. Also, the propellant behavior departs dramatically from linear viscoelasticity once the peak stress is passed; the linear prediction shows a much higher stress than is actually observed. This departure from the linear prediction may not be important in predicting failure, however.

3. ANALYSIS DETAILS

The analysis was done using a Hewlett-Packard 9815A programmable calculator. During this study several programs, discussed later, were devised to perform different calculations during the study. Two methods of approximating a smooth strain time history were compared: approximation by a series of steps and approximation by a series of ramps. The smooth curve used was a fourth-order polynomial.

3.1 Overall Approach

The calculator programs developed and their use are described below.

3.1.1 Power Law Modulus Program - The Power Law Modulus Program was written to calculate constants for a modified power law modulus equation applicable to an isothermal loading situation, using given relaxation modulus data as a function of time. The program forces the power law to fit three points $[\xi_i, E_r(\xi_i)]$ where ξ is the "reduced time" t/a_T, and E_r is relaxation modulus.

The power law equation is

$$\left(\frac{T_s}{T}\right) E_r = \tilde{E}_r = [E_o (\xi)^n + E_\infty]. \tag{1}$$

Let

$$\hat{E}_r = E_r \Big|_{T = \text{const}}, \qquad \hat{E}_o = \left(\frac{T}{T_s}\right) \frac{E_o}{(a_T)^n},$$

and

$$\hat{E}_\infty = \left(\frac{T}{T_s}\right) E_\infty;$$

then

$$\hat{E}_r = \hat{E}_o (t)^n + \hat{E}_\infty . \tag{2}$$

Equation 1 can be solved for three different points $[\xi_i \; (\tilde{E}_r)_i]$ to yield:

$$\log_{10} E_o = \frac{\{(\log_{10}\xi_2)[\log_{10}(\tilde{E}_{r_1} - E_\infty)] - (\log_{10}\xi_1)[\log_{10}(\tilde{E}_{r_2} - E_\infty)]\}}{(\log_{10}\xi_2 - \log_{10}\xi_1)} \tag{3}$$

$$n = \frac{\log_{10}(\tilde{E}_{r_2} - E_\infty) - \log_{10} E_o}{\log_{10}\xi_1} \tag{4}$$

and

$$E_\infty = \tilde{E}_{r_3} - E_o \xi_3^n . \tag{5}$$

Equations 3, 4 and 5 are solved in the calculator program by iterating on an assumed value of E_∞. The value of E_∞ converges quickly to within 1×10^{-6} psi.

3.1.2 "Polynomial" Program - In this program the "hereditary integral" is evaluated for a polynomial strain history given a modified power law representation of the linear viscoelastic relaxation modulus. The program then calculates the strain history and stress response.

The program first determines the constants in the polynomial

$$\varepsilon(\tau) = \sum_{m=1}^{4} c_m \tau^m \tag{6}$$

where τ is the time variable describing the strain history. The constants are determined from user input values of (t,ε) at the point of maximum strain rate and (t,ε) at the point of maximum strain. The stress at time t is given by the hereditary integral:

$$\sigma(t) = \int_0^t E_r(t-\tau)\frac{d\varepsilon}{d\tau}\, d\tau$$

or

$$\sigma(t) = \int_0^t \hat{E}_o (t-\tau)^n \frac{d\varepsilon}{d\tau}\, d\tau + E_\infty \varepsilon(t) \tag{7}$$

Evaluation of this integral using Equation 6 for the strain history results in

$$\sigma(t) = \sum_{m=1}^{4} \Delta\sigma_m + \hat{E}_\infty \varepsilon \qquad (8)$$

where

$$\Delta\sigma_m = \left[\prod_{j=0}^{m-1} \left(\frac{m-j}{m+n-j}\right)\right] (c_m \hat{E}_o t^{(m+n)}). \qquad (9)$$

Equations 6, 8 and 9 are implemented in subroutines which are also used in the programs discussed in Sections 3.1.3 and 3.1.4.

The calculator program prints out time, strain, and stress at time defined by a user-input maximum time and number of increments.

3.1.3 Stepwise Approximation Program. - This program calculates a stepwise approximation to the polynomial strain history, evaluates the hereditary integral to obtain the stress response, and calculates root-mean-square (rms) errors for the strain history and stress response as compared to those (the "exact" values) for the polynomial. Subroutines from the "Polynomial" program are used to calculate the "exact" stress and strain values.

The power law used is Equation 2. The hereditary integral, equation 7, when evaluated at time t_j during the j^{th} step, becomes

$$\sigma(t) = \sum_{i=1}^{j} E_o(t_j - \tau_i)^n (\Delta\varepsilon)_i + E_\infty(\varepsilon_p)_{\tau_j} \qquad (10)$$

where

$$\Delta\varepsilon_i = (\varepsilon_p)_{\tau_1} + K_\varepsilon[(\varepsilon_p)_{\tau_{i+1}} - (\varepsilon_p)_{\tau_i}] \qquad (11)$$

and $\quad t_j = \tau_j + K_\sigma\ (\tau_{j+1} - \tau_j)$ (12)

and where $(\varepsilon_p)_t$ refers to the strain given by the polynomial (Eq 6) at time t; τ_i is the time at which the i^{th} step occurs; and the parameters K_ε and K_σ are defined pictorially in Figure 1. (While Figure 1 shows the actual strain history as a ramp function, the definition of K_ε and K_σ are independent of the actual strain history.) Variations in K_ε and K_σ allow different schemes for defining the stepwise strain history (given a "real" continuous history) and computing a corresponding stress history.

The program implements Equations 10, 11, and 12, calculates the rms relative error in strain at m evenly spaced points in the strain history (relative to the polynomial history) and calculates the rms relative error in the step-response stresses relative to the "exact" polynomial-history response (only the stress values at times t_j are considered). The user controls the number of steps (NSTEPS) and the parameter m as well as K_ε and K_σ.

3.1.4 Piecewise-linear Approximation Program - This program calculates a piecewise-linear approximation to the polynomial strain history, evaluates the hereditary integral, and calculates rms relative errors for the strain history and stress response. Subroutines from the "Polynomial" program are implemented to calculated exact stress and strain values.

The power law used is Equation 2. The hereditary integral, Equation 7, when evaluated at time t_j during the jth step, becomes:

$$\sigma(t) = \sum_{i=0}^{j} \frac{\hat{E}_o R_i (t_j - \tau_i)^{n+1}}{n+1} + E_\infty(\varepsilon_p)_j \qquad (13)$$

where

$$R_i = \frac{[(\varepsilon_p)_{\tau_{i+1}} - (\varepsilon_p)_{\tau_i}]}{(\tau_{i+1} - \tau_i)} - \sum_{k=1}^{i-1} R_k \qquad (14)$$

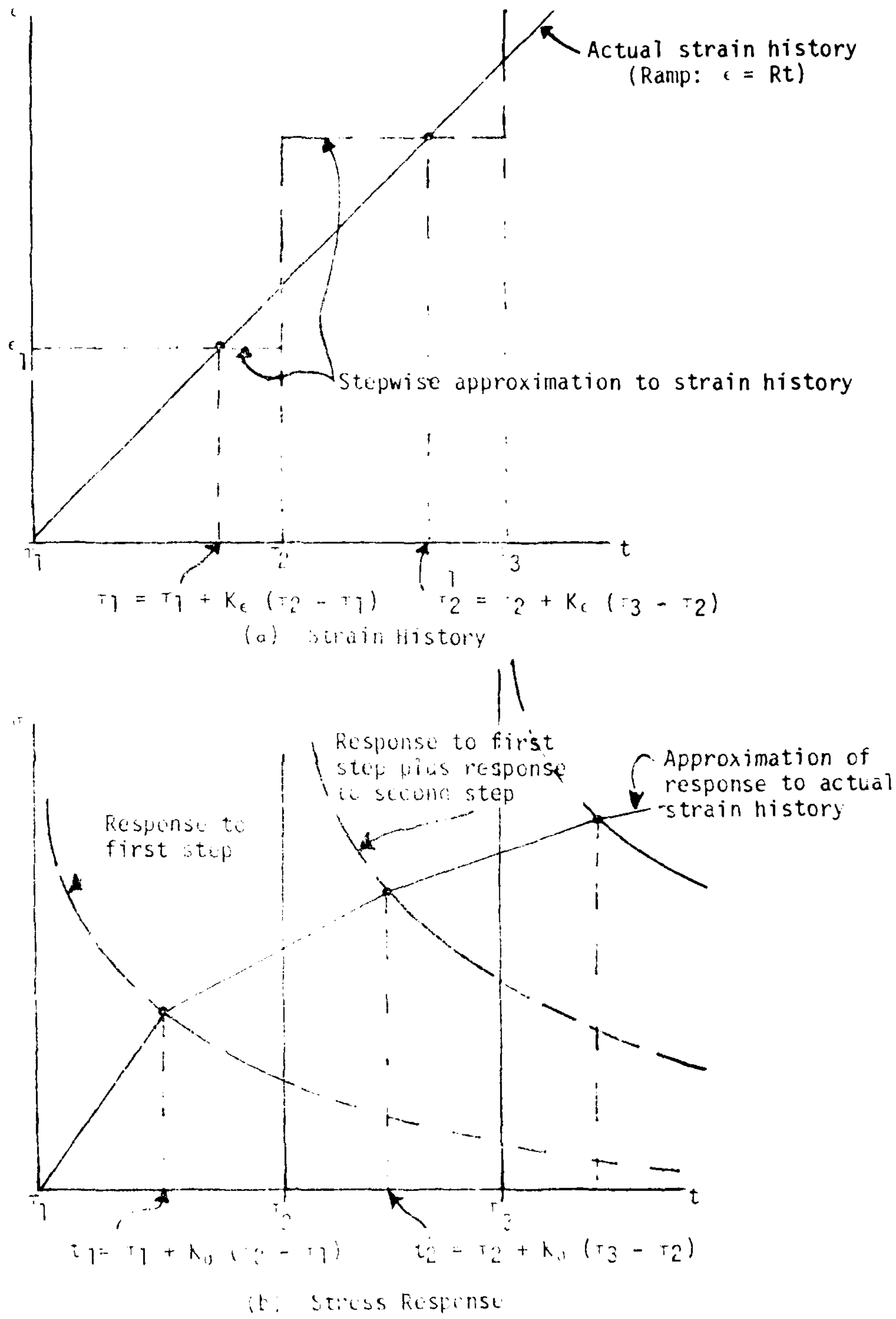

Figure 1. Step Approximation to Ramp Strain History.

and

$$t_j = \tau_j + K_\sigma (\tau_{j+1} - \tau_j) \tag{15}$$

where $(\epsilon_p)_t$ refers to the strain given by the polynomial (Equation 6) at time t, τ_j is the time at which the jth ramp begins, and the parameter K_σ is defined in Figure 2.

The program implements Equations 13, 14 and 15. The strain history and stress response errors are calculated the same way as in the stepwise approximation program (Section 3.1.3). The user inputs the number of steps (NSTEPS), the parameter m, and K_σ.

3.1.5 Application of Programs - The programs described in Sections 3.1.3 and 3.1.4 were used first to find the optimum values of K_ϵ and K_σ for approximating a ramp (taken as apolynomial with zero constants except for the linear term) with steps, and then to find the optimum value of K_σ for approximating the polynomial strain history with ramps. Finally, the performance of stepwise approximations to the polynomial and piecewise-linear approximations to the polynomial were compared to select the best way of approximating an arbitrary history. The piecewise-linear approximation was found to be best. These calculations are discussed in detail in Sections 3.2 and 3.3.

Finally, a new program, "Ramp-Series Stress Response for Arbitrary Load History," was written to calculate a piecewise-linear approximation to an arbitrary strain history and to the corresponding stress response. The new program is very similar to the "Piecewise-linear Approximation Program." The primary differences are that the new program uses a discrete table of time and strain values instead of the polynomial history, and that it does not contain the error calculations. This new program was applied to an actual strain history from data reported in AFRPL-

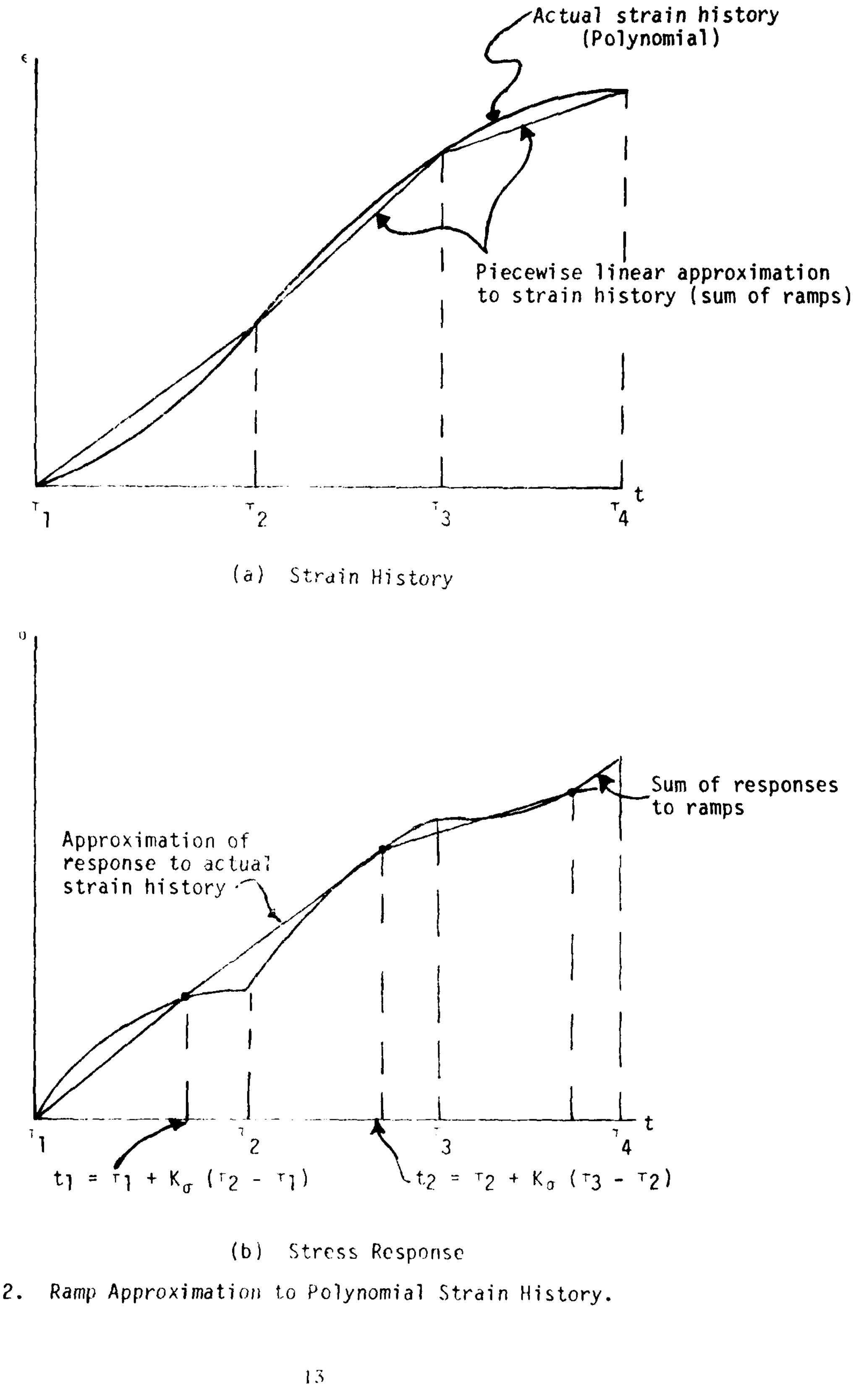

Figure 2. Ramp Approximation to Polynomial Strain History.

TR-78-68, "Improved Solid Propellant Mechanical Properties Measurement for Structural Analysis Input." The resulting stress history, as well as the stress history resulting from a polynomial strain history which closely matches the actual strain history, were compared with the actual measured stress history. These results are discussed in Section 3.4.

3.2 Calculations for Ramp Strain History

An arbitrary modulus law (Equation 2) was used with $\hat{E}_o = 2.3859 \times 10^3$ psi (16.450 MPa), $\hat{E}_\infty = 55.408$ psi (0.38202 MPa), and $n = -0.32790$, with t in minutes (for t in seconds, the value of $\hat{E}_o$ would be 623.16 psi (4.297 MPa)). The Stepwise Approximation Program was used with a ramp substituted for the polynomial ($C = 21.923$, $C_2 = C_3 = C_4 = 0$, for t in minutes; $C_1 = 0.36538$, $C_2 = C_3 = C_4 = 0$ for t in seconds).

Figure 3 shows the ramp strain history and the resulting "exact" stress response used in this part of the study.

Initial runs with the Stepwise Approximation Program were made using selected values of the parameters K_ε, K_σ, and NSTEPS as shown in Table 1. The results (shown in Figures 4-6) show the rms stress error as a function of K_σ for K_ε = 0, 0.5, and 1.0 (these K_ε values were chosen because they are simple to use for evenly spaced time intervals when the data is available only in discrete form). Additional runs were made to search out the optimum (i.e., least-error) value of K_σ for each K_ε . The best results were obtained with $K_\varepsilon = 0.5$ and $K_\sigma = 0.35$. Interestingly, it can be shown that, for a single step approximating a ramp over the time interval τ_m, the value of K_σ which yields identical stresses for the ramp and the step (for $K_\varepsilon \neq 0$) is

$$K_\sigma^* = K_\varepsilon \left[\frac{\hat{E}_o (K_\sigma^* \tau_m)^n + \hat{E}_\infty}{\dfrac{\hat{E}_o (K_\sigma^* \tau_m)^n}{(n+1)} + \hat{E}_\infty} \right]$$

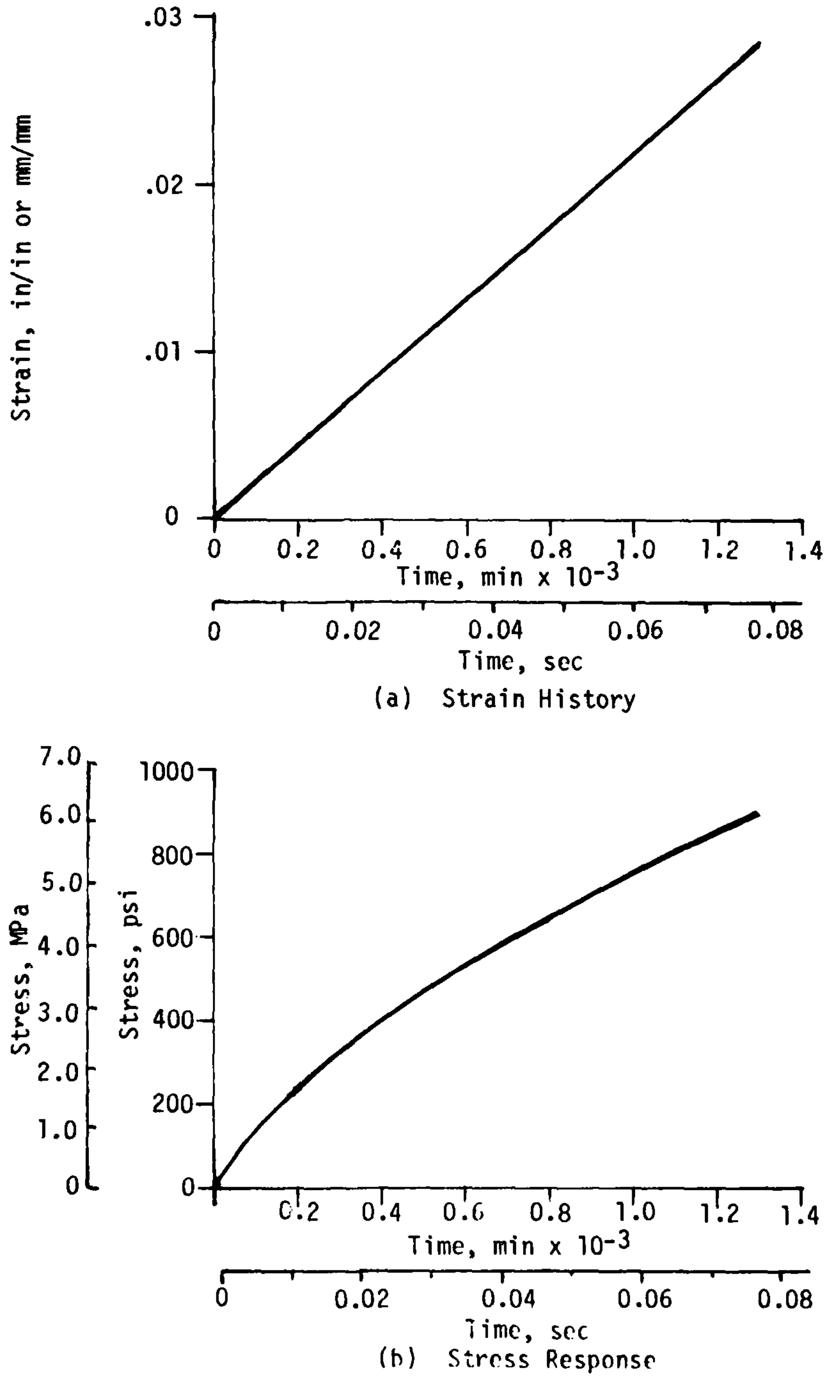

Figure 3. Ramp Strain History and "Exact" Stress Response.

TABLE 1. MATRIX OF PARAMETERS FOR INITIAL "RAMPS" CALCULATIONS

N STEPS	100	30	10	3	1
$K_\epsilon = .5$					
$K_\sigma = .25$		X			
$K_\sigma = .5$	X	X	X	X	X
$K_\sigma = .75$		X			
$K_\sigma = 1.0$		X			
$K_\epsilon = 0$					
$K_\sigma = .25$		X			
$K_\sigma = .5$	X	X	X	X	X
$K_\sigma = .75$		X			
$K_\sigma = 1.0$		X			
$K_\epsilon = 1$					
$K_\sigma = .25$		X			
$K_\sigma = .5$	X	X	X	X	X
$K_\sigma = .75$		X			
$K_\sigma = 1.0$		X			

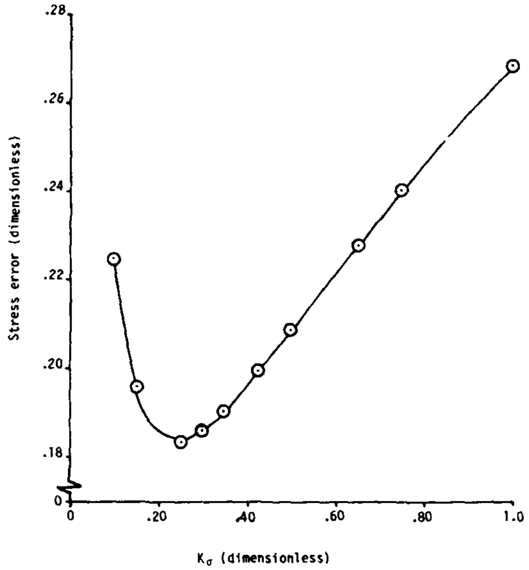

Figure 4. Variation of Stress Error with K_σ for $K_\varepsilon = 0$ (Step Approximation to Ramp, 30 Time Intervals).

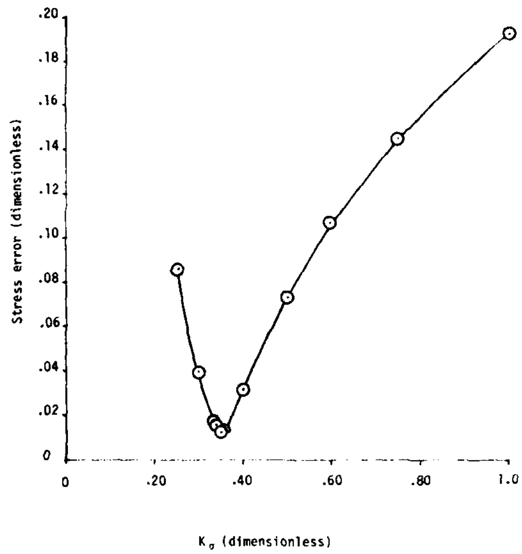

Figure 5. Variation of Stress Error with K_σ for $K_\varepsilon = 0.5$ (Step Approximation to Ramp, 30 Time Intervals).

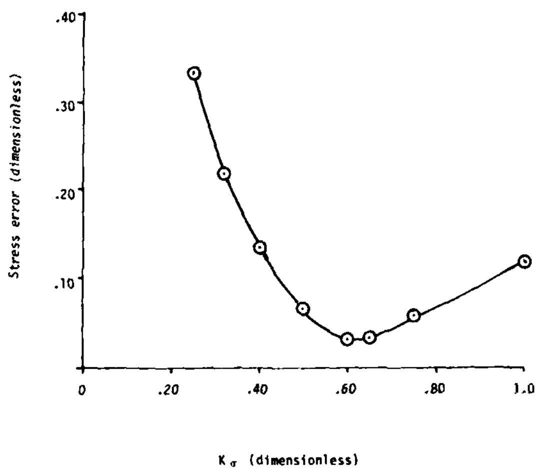

Figure 6. Variation of Stress Error with K_σ for $K_\varepsilon = 1.0$ (Step Approximation to Ramp, 30 Time Intervals).

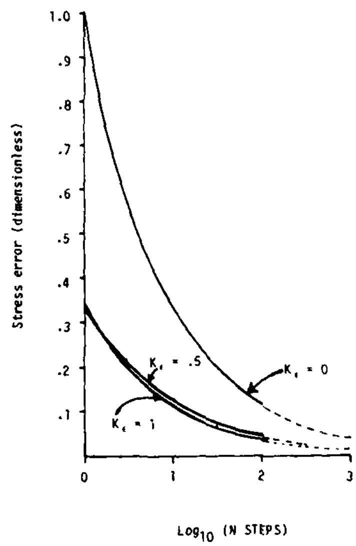

Figure 7. Variation of Stress Error with Number of Time Intervals for $K_\sigma = 0.5$ (Step Approximation to Ramp)

For τ_m = 1.3 x 10^{-3} and the modulus law constants used in the study, this equation yields K_σ^* = 0.674 K_ϵ , which agrees fairly closely with the results in Figures 5 and 6. The optimum value of K_σ may therefore be a function of the modulus constants. This factor was not explored further in the study.

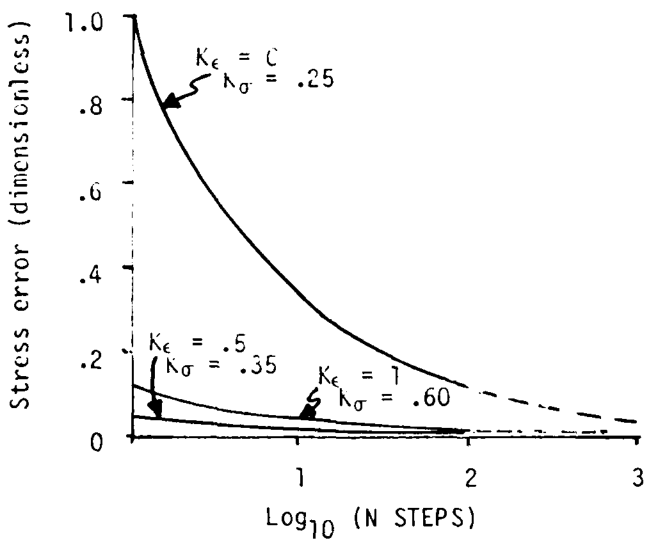

Figure 8. Variation of Stress Error with Number of Time Intervals for K_σ = .35 (Step Approximation to Linear Ramp).

Figures 7 and 8 show the variation of stress error with NSTEPS. As can be verified by a log-log plot of the variables, the stress error varies as $1/\sqrt{NSTEPS}$, so that the user pays a heavy price in computation time to improve accuracy by increasing the number of steps. It is obvious from these figures that using either K_σ = 0.5 or K_ϵ = 1.0 is vastly preferable to using K_ϵ = 0, and that using the optimum value of K for each K_ϵ provides a substantial improvement in the stress error in comparison to an arbitrary value of K_σ = 0.5.

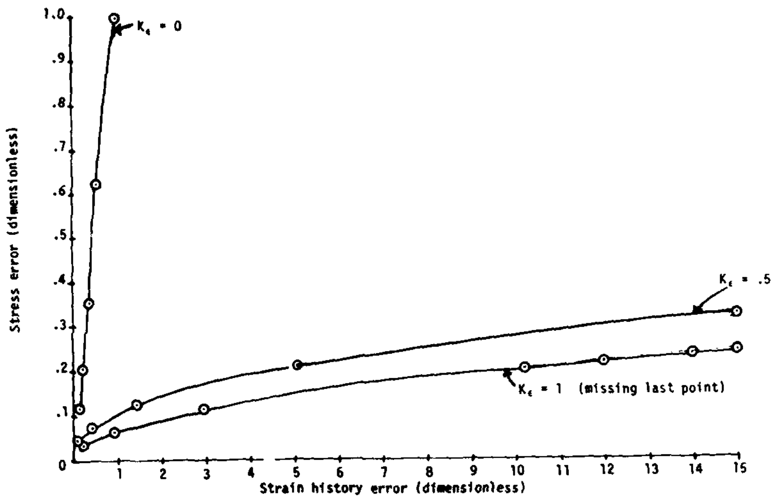

Figure 9. Variation of Stress Error with Strain History Error for $K_\sigma = 0.5$ (Step Approximation to Ramp).

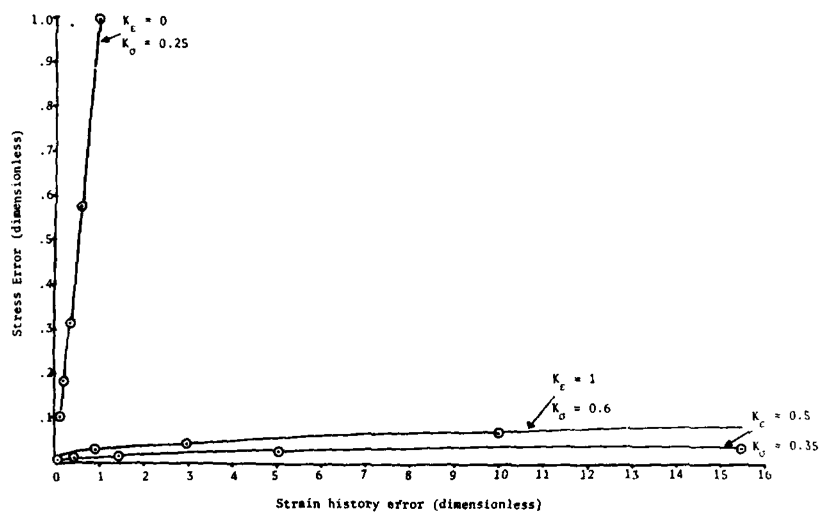

Figure 10. Variation of Stress Error with Strain History Error for Optimum K_σ (Step Approximation to Ramp).

Figures 9 and 10 show the variation of stress error with strain history error; the improvement provided by the optimum K_σ values is again clearly evident.

The lowest error is obtained using $K_\epsilon = 0.5$ and the corresponding value of K_σ ($K_\sigma = 0.35$). These values were selected for use in the continued study described in the following section.

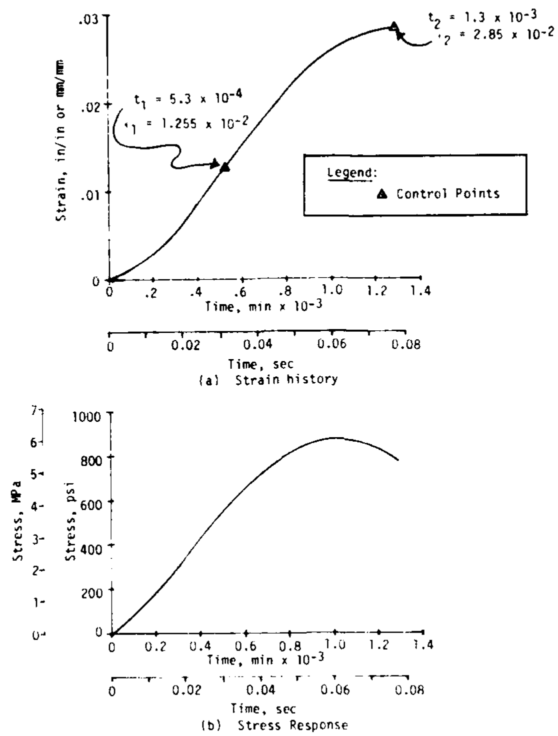

Figure 11. Polynomial Strain History Used in Study.

3.3 Calculations For Polynomial Strain History

The arbitrary modulus law (Eq 2) used in the calculations for a ramp strain history and the constants $\hat{E}_0$, $\dot{E}_\infty$, and n are given in Section 3.2 were also used in this part of the study.

The Piecewise-linear Approximation Program was used with a polynomial strain history. The constants were determined, using the control points shown in Figure 11a, with the "Polynomial" program. The resulting constants are:

(Time in Minutes)	(Time in Seconds)
$C_1 = 2.7549$	$C_1 = 1.6529 \times 10^2$
$C_2 = 6.3493 \times 10^4$	$C_2 = 2.2857 \times 10^8$
$C_3 = -5.0683 \times 10^7$	$C_3 = -1.0948 \times 10^{13}$
$C_4 = 1.0142 \times 10^{10}$	$C_4 = 1.3144 \times 10^{17}$

The resulting "exact" stress response is shown in Figure 11b.

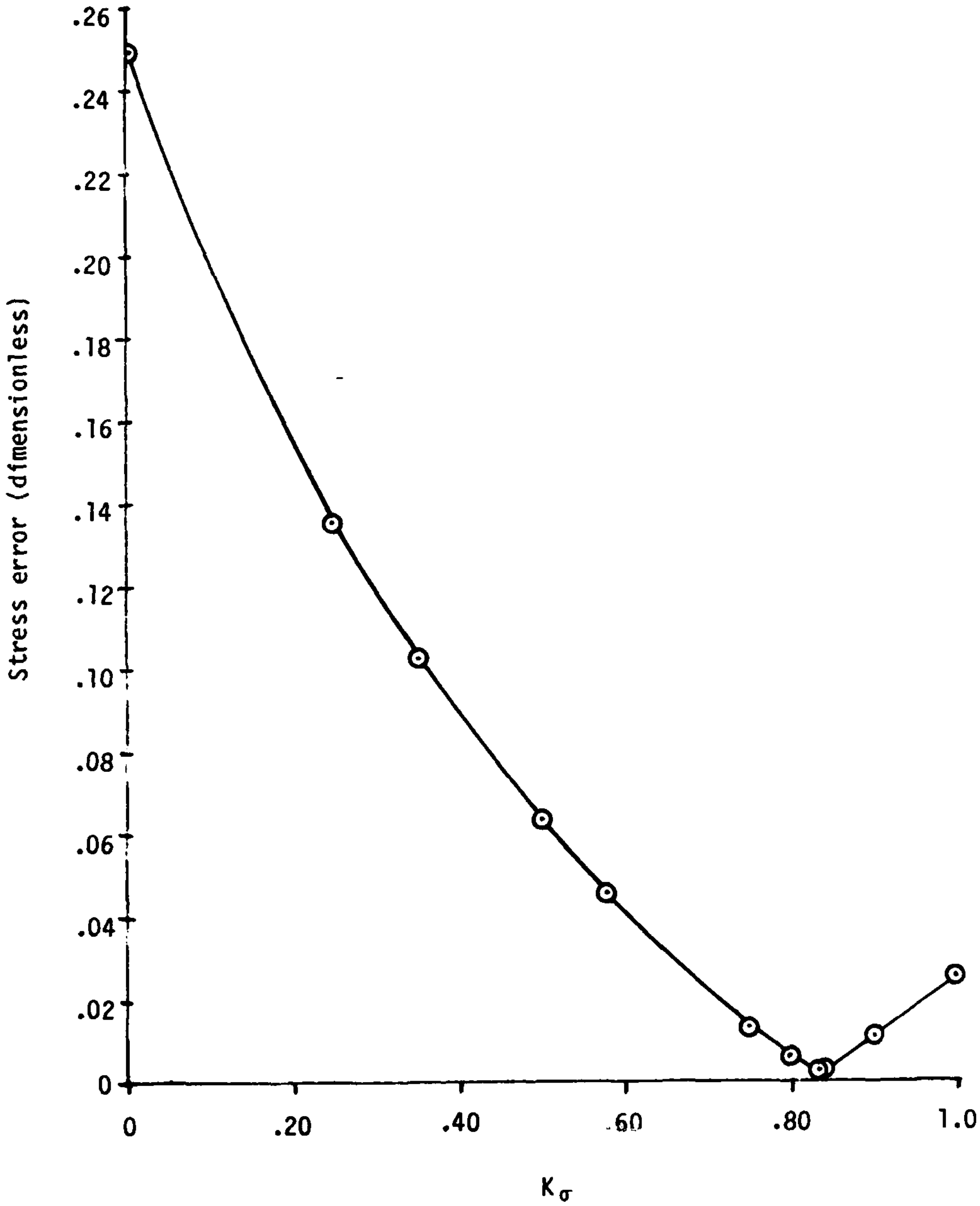

Figure 12. Variation of Stress Error with K_σ (Ramp Approximation to Polynomial, 30 Time Intervals)

Initial runs with the Piecewise-linear Program were made using selected values of the parameters K_σ and NSTEPS as shown in Table 2. The results are shown in Figure 12.

TABLE 2. MATRIX OF INITIAL K_σ VALUES USED IN PIECEWISE-LINEAR ANALYSES					
K_σ	.001	.25	.5	.75	1.0
NSteps = 30	X	X	X	X	X

Additional runs (Table 3) were made to search out the optimum (i.e., least-error) value of K_σ. The best result was obtained at K_σ = .833.

TABLE 3. MATRIX OF ADDITIONAL ANALYSIS PARAMETERS					
N STEPS	100	30	10	3	1
(Ramps) K_σ = .833	X	X	X	X	X
(Ramps) K_σ = .5	X	X	X	X	X
(Steps) K_ϵ = .5 K_σ = .5	X	X	X	X	X
(Steps) K_ϵ = .5 K_σ = .5	X	X	X	X	X

Based on the discussion in Section 3.2, the optimum value of K_σ is probably dependent on the modulus constants. This study did not explore this factor further.

Figure 13 (based on the results of the additional runs indicated in Table 3) shows the piecewise-linear approximation is superior to the stepwise approximation. The piecewise-linear approximation has a much lower stress error for any combination of NSTEPS and the controlling parameter K_σ which forces the stepwise program's error below 5%. For example, using optimum values of K_σ, the piecewise-linear approximation with NSTEPS = 10 yields a lower error than

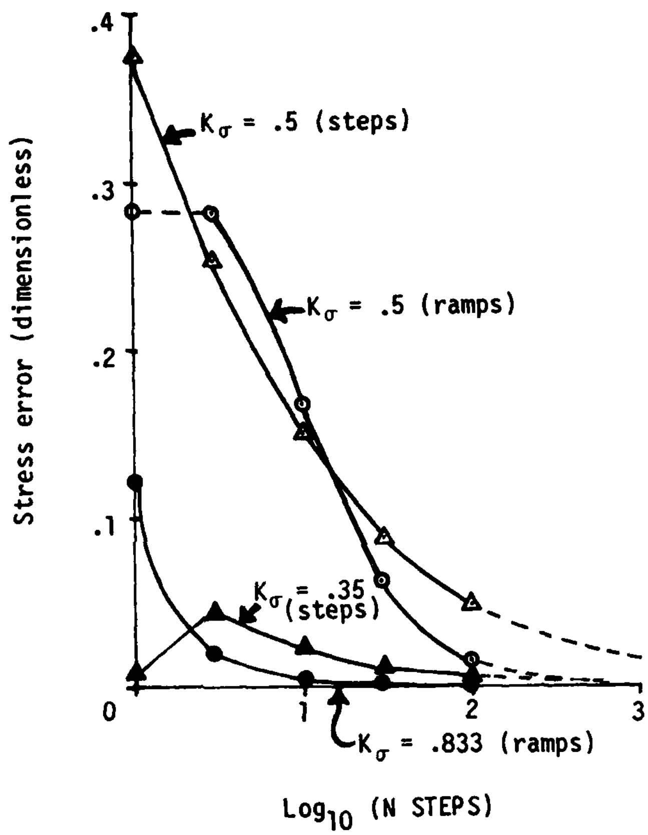

Figure 13. Variation of Stress Error with Number of Time Intervals (Ramp and Step Approximations to Polynomial).

using the stepwise approximation with NSTEPS - 100. If an rms error of 0.5% is acceptable in the stress response, then a value of NSTEPS = 10 should be sufficient in a piecewise-linear approximation of a general strain history.

3.4 Application to Actual Data

AFRPL-TR-78-68, "Improved Solid Propellant Mechanical Properties Measurement for Structural Analysis Input" (Thiokol/Huntsville, September 1978), reports the results of dynamic tests of propellant samples under simulated motor ignition conditions. In these tests propellant samples were immersed in a temperature-conditioned fluid and held at a predetermined strain level to simulate motor storage thermal loads. The fluid was then pressurized with gas, providing a transient pressure history similar to a motor ignition pressurization. The test equipment was arranged so that the pressurized fluid drove the test machine ram downward against the resistance of steel springs (as well as the propellant sample's resistance and the inertia of moving parts). The result was a transient strain history that simulated the strain at the inner bore of a rocket motor undergoing ignition pressurization.

Since the stress-strain data for some of these tests was reported, along with conventional relaxation test data, an ideal test case was provided for the techniques studied in the present effort. Figure 14 is a photograph of the oscillograph ("strip chart") data (Figure 9 in AFRPL-TR-78-68). This data corresponds to Run No 1 in Table F-5 of AFRPL-TR-78-68. The prestrain level for the tests was zero. Other test parameters and results given in Table F-5 of AFRPL-TR-78-68 were:

Temperature:	-65°F (-53.9°C)
Maximum Pressure:	1310 psi (9.03 MPa)
Time to Maximum Pressure:	67.9 ms
Strain at Maximum Pressure	0.0317 in/in (.0317 mm/mm)
Stress at Maximum Pressure:	732 psi (5.05 MPa)

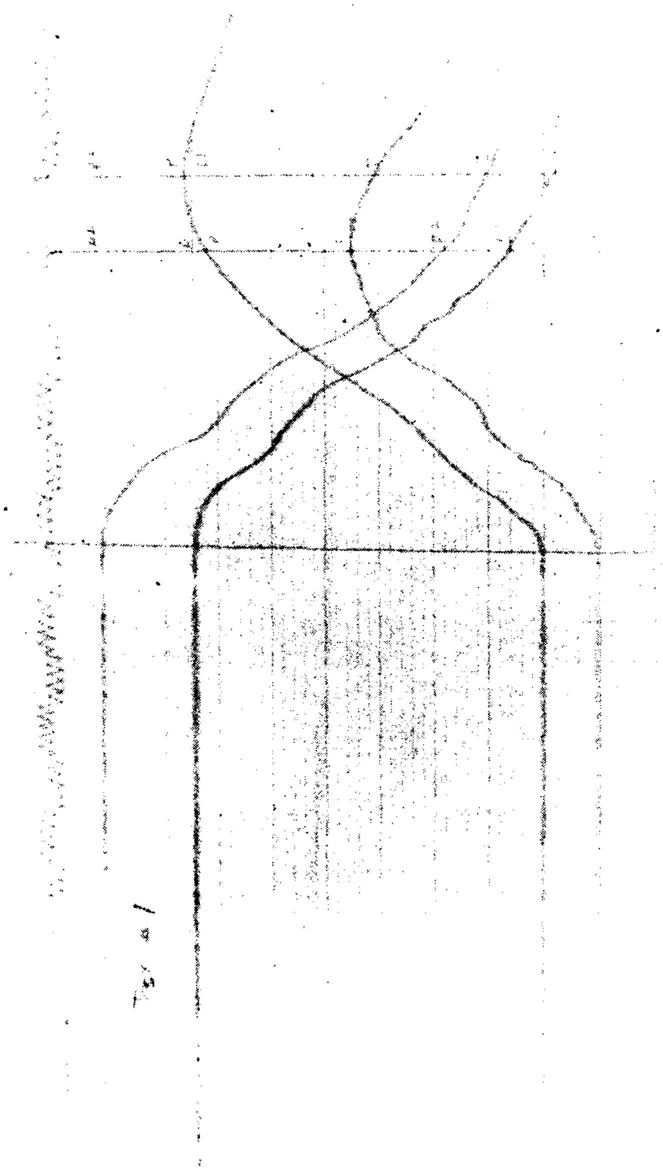

Fig. 1

These values were used to scale the data shown in Figure 14. In scaling the displacement traces the amplitude of both D_1 and D_2 were taken as 0.0317 in/in (0.0317 mm/mm); the resulting scaled strains were then averaged. The scaled data is given in Figures 15 and 16. (A careful examination of Figure 14 will reveal that the image is distorted, presumably by perspective effects in the photography. An effort was made to accurately account for the distortion in scaling the data.)

Comparison of Figure 15 with Figure 16(a) shows that the strain history lags the pressure history somewhat but otherwise corresponds fairly closely. The strain history has the same general appearance as the polynomial history shown in Figure 11 (up to the peak value), except for an added oscillation or "bumpiness", which appears even more strongly in the stress history (Figure 16(b)).

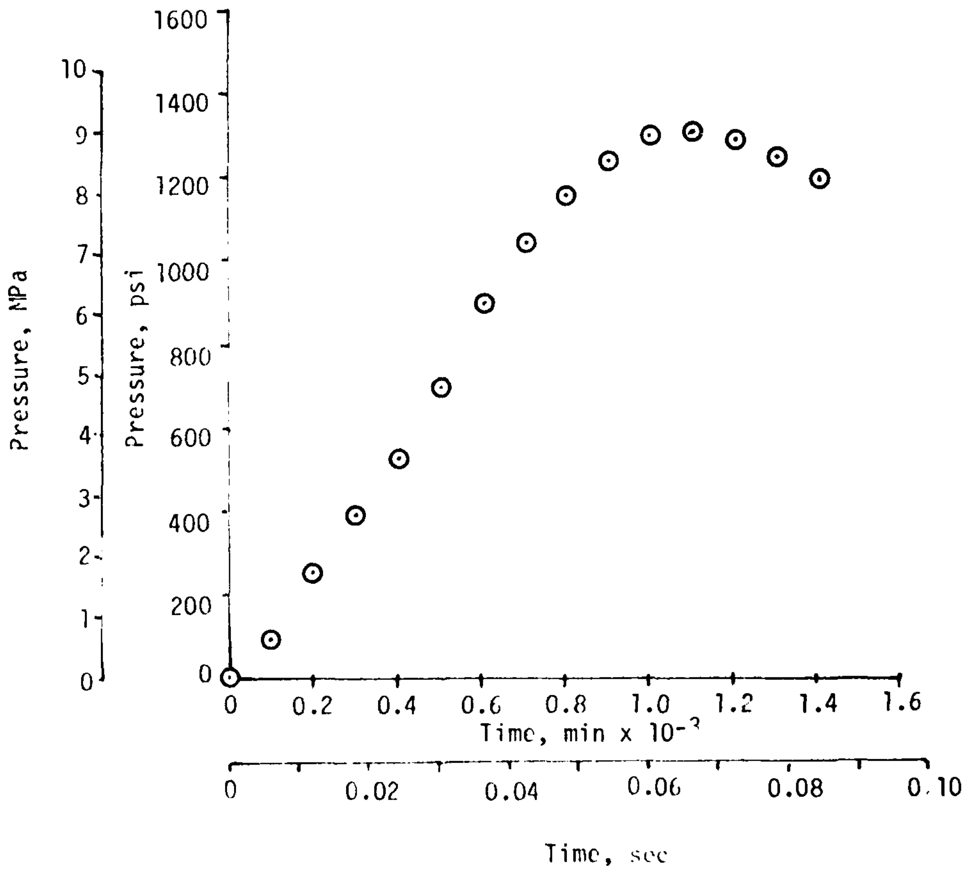

Figure 15. Pressure-Time History Scaled from Strip Chart.

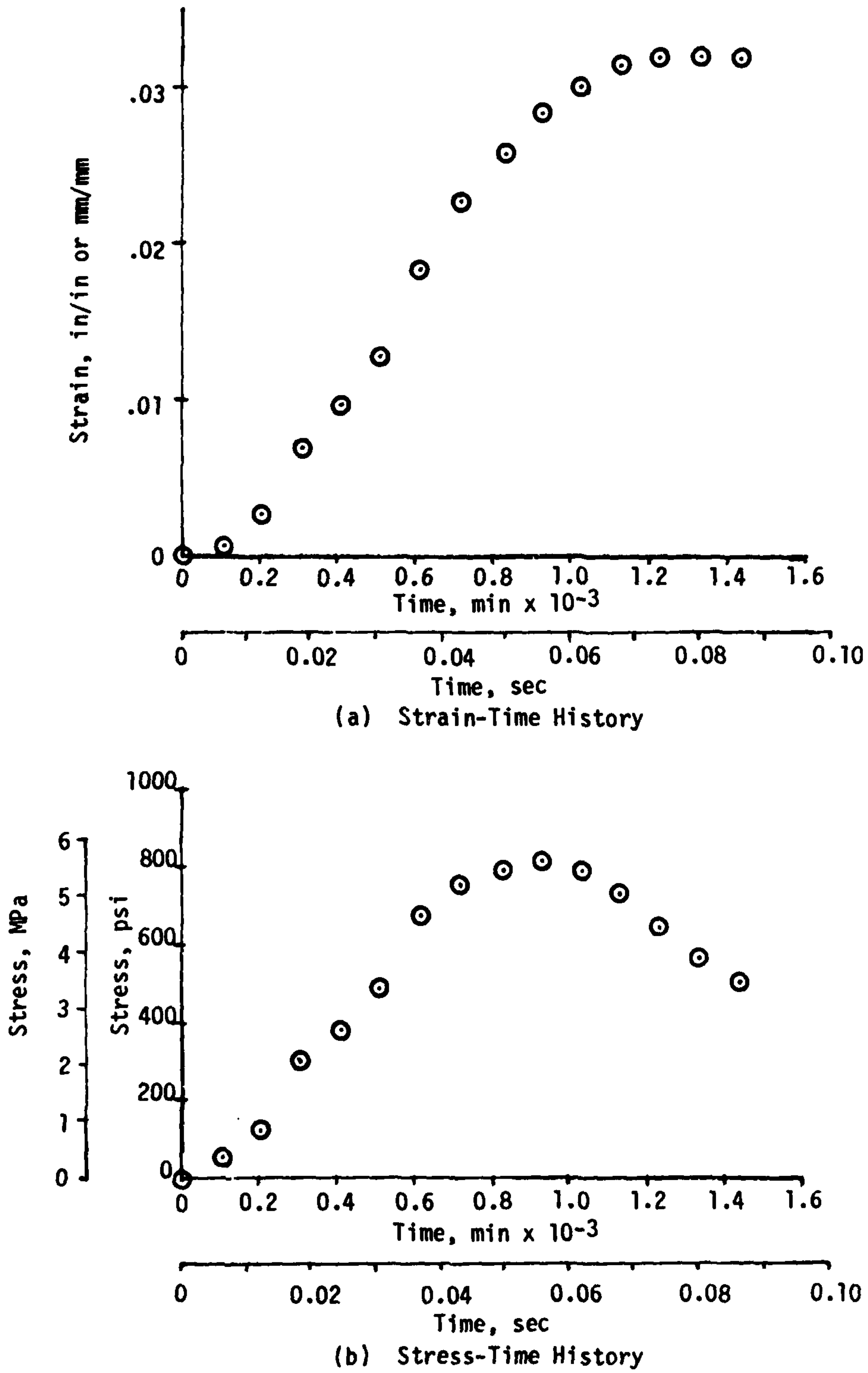

Figure 16. Strain and Stress Data Scaled from Strip Chart.

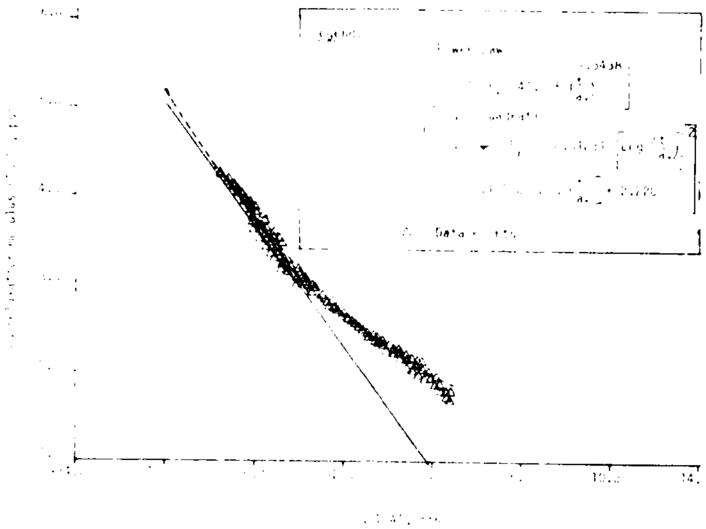

Power Law
Data Points
10.0

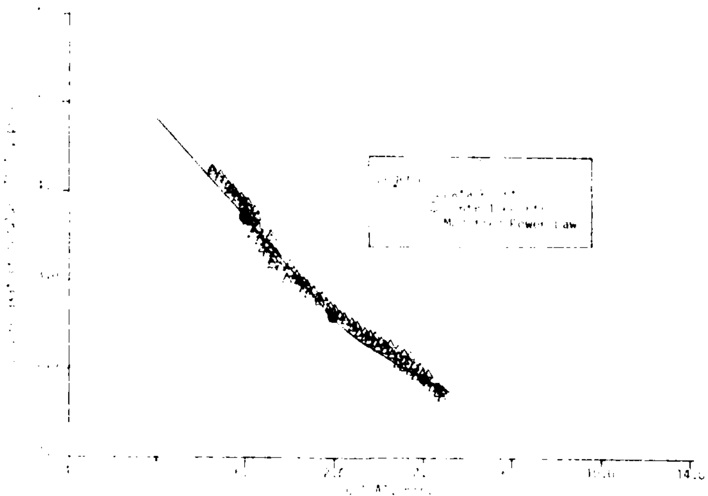

Power Law
10.0
14.0

The relaxation modulus for this propellant was determined at several different strain levels. The data reported for 2.5% strain as well as two different analytical representations is shown in Figure 17. The power law and the log-quadratic equations are tangent at the $\log_{10}(t/a_T) = -7$ point (with t/a_T in minutes). While the combination of these two functions fits the data well over the entire range of data, the log-quadratic function produces a hereditary integral which must be numerically evaluated for any strain history other than a step function. In practice, the power law is the only part of the combination involved in evaulating propellant response under the loading conditions of interest in this report because only reduced times less than 10^{-7} minutes are involved. It was felt that the Thiokol power law had a higher slope than was supported by the data, so two alternative modified power laws were determined using the Power Law Modulus Program discussed earlier. These alternative representations are "Modified Power Law Number 1", shown in Figure 18, and "Modified Power Law Number 2", shown in Figure 19. The difference between these two representations is in the center control point (the modulus equation was forced through the three points shown in each figure). The modulus constants (for a temperature of -65°F (-53.9°C)) determined for the modified power law equation (Eq. 2) for the English system of units (modulus in psi, t/a_T in minutes) are:

	$\hat{E}_o$, psi	$\hat{E}_\infty$, psi	n (dim)
Modified Power Law No 1	2497	38.8	-0.28252
Modified Power Law No 2	2426	44.9	-0.30382

For the SI system of units (modulus in MPa, t/a_T in seconds), the constants are:

	$\hat{E}_o$, psi	$\hat{E}_\infty$, MPa	n (dim)
Modified Power Law No 1	54.74	0.268	-0.28252
Modified Power Law No 2	58.03	0.310	-0.30382

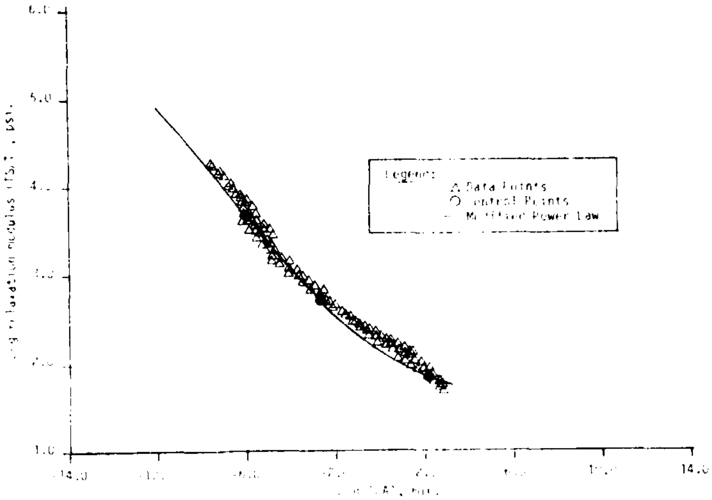

The two modified power law representations are related to the relaxation data by the WLF shift factor (a_T) equation.

$$\log_{10} a_T = \frac{-7.511(T - 298)}{188.5 + (T - 298)} \qquad (16)$$

which was determined by Thiokol specifically for the relaxation data in Figures 17, 18, and 19. In this equation, T is in K. The calculations in this report use a value of 298.15 where the value 298 appears in Equation 16: this corresponds to a reference temperature (for which $\text{Log } a_T = 0$) of 77°F or 25°C.

Examination of Figures 18 and 19 shows that "Modified Power Law Number 2" agrees better with the measured data at very short times ($t/a_T < 10^{-2}$ min), while Modified Power Law Number 1 agrees better with the data for longer reduced times. We are concerned with reduced times shorter than 10^{-8} minutes, so "Modified Power Law Number 2" appears preferable to "Modified Power Law Number 1." "Modified Power Law Number 2" also appears to be more consistent with the relaxation data than does the Thiokol power law.

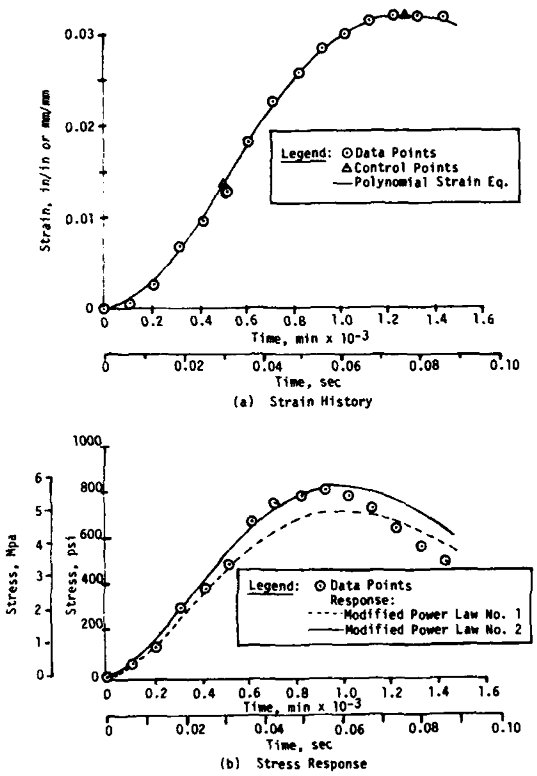

Figure 20. Polynomial Strain History Results.

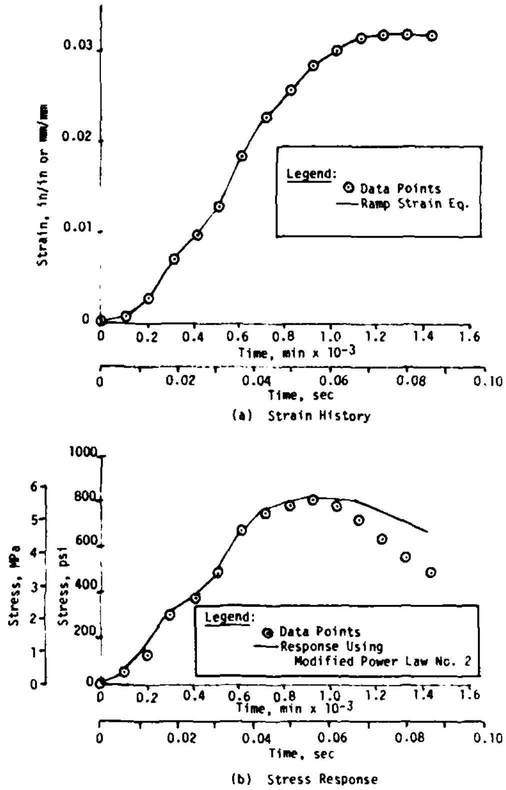

Figure 21. Piecewise-Linear Strain History Results.

The strain histories considered are shown in Figures 20(a) and 21(a). The data points plotted as circles were scaled from Figure 14 using strain at maximum pressure to determine scale factors.

The polynomial strain history was forced through a point of inflection and a maximum at the control points shown in Figure 20(a). The resulting constants in Equation 6 were:

Time in Minutes	Time in Seconds
$C_1 = 5.5035 \times 10^2 \ (\text{min})^{-1}$	$C_1 \approx 9.1725 \times 10^{-4} \ (\text{sec})^{-1}$
$C_2 = 8.8909 \times 10^4 \ (\text{min})^{-2}$	$C_2 = 24.697 \ (\text{sec})^{-2}$
$C_3 = -7.7605 \times 10^7 \ (\text{min})^{-3}$	$C_3 = -3.5928 \times 10^2 \ (\text{sec})^{-3}$
$C_4 = 1.8332 \times 10^{10}$	$C_4 = 1.4145 \times 10^3 \ (\text{sec})^{-4}$

The resulting stress responses are shown in Figure 20(b), along with the stress data (circles) scaled from Figure 14, for both "Modified Power Law Number 1" and "Modified Power Law Number 2". As expected, "Modified Power Law Number 2" agrees better with the data. Notably, the "bumpiness" seen in the data is not captured in the stress response (the polynomial strain history smooths through the "bumps" in the strain history). The calculated stress for "Modified Power Law Number 2" agrees quite well with the measured stress through the maximum measured stress point. However, once the stress begins to decrease, the calculated viscoelastic response fails to drop off as quickly as the measured stress. By the time of peak pressure at $t = 1.13 \times 10^{-3}$ min (67.9 msec) the calculated stress is [illegible]% higher than the measured stress.

A piecewise-linear strain history was constructed through the data points from Figure 14, as shown in Figure 21(a). The value of K_η used (see Equation 15 and Figure 2) was 0.833 (this value was found to produce minimum root mean square error in the study discussed in Section 3.3, which used a similar strain history and modulus constants). The results were essentially identical to those for the polynomial strain history, except that the calculated stress response followed the "bumps" seen in the actual data.

Based on the results, we observe that:

(1) "Modified Power Law Number 2" is a good approximation to the linear viscoelastic modulus at high rates (although we had to extrapolate beyond the range of measured data for the problem at hand).

(2) Linear viscoelasticity (based on the limited data available) appears to accurately predict stress response to a transient strain history <u>without a prestrain</u>, although stresses beyond the time of actual peak stress are overpredicted. (Some damage effects may be the cause of the more rapid drop-off in measured stress). The error at peak stress for both the polynomial and piecewise linear strain history approximations is less than 20 psi of the measured value of 810 psi, or less than 2.5%.

4. CONCLUSIONS AND RECOMMENDATIONS

This successful analysis effort fully met the objectives. Some innovative approaches to the analysis of propellant viscoelastic response under motor ignition pressurization conditions were developed, and a number of useful calculator programs were created for AFRPL in-house use.

We recommend that the techniques developed in this program be extended to the more difficult problem of thermal transient loading with coupled strain and temperature histories. We also recommend that the techniques be applied to problems involving prestrain to determine whether prestrain causes the linear approach to fail.